ELEVATED TEMPERATURE CRACK GROWTH IN A LOW ALLOY STEEL DUE TO MAJOR AND MINOR STRESS CYCLES

M Hawkyard* and B E Powell*

Fatigue crack growth rates have been measured at 400°C in corner notched specimens of 817M40 wrought steel. The fatigue loadings consisted of major cycles with a stress ratio of 0.1 and minor stress cycles with a stress ratio of 0.9, either applied separately or in combination. When applied separately, the major cycles generated a bi-linear fatigue crack growth curve, whilst the minor cycles gave threshold values and near-threshold growth rates which were dependent on the test method employed. Under the conjoint action of major and minor stress cycles, the expected form of growth rate curve was observed but not accurately predicted by the linear summation model.

INTRODUCTION

Studies of the effects of combined cycle fatigue (CCF) involving the conjoint action of major and minor stress cycles have concentrated on the fatigue crack growth (FCG) behaviour of titanium and nickel alloys (1,2). But steels are also used under loading conditions which involve a mixture of large amplitude, low-frequency major stress cycles and low-amplitude, high-frequency minor stress cycles. The loading of particular interest is a simple representation of both the start-stop cycles and the possible in-service vibrations associated with the operation of many machines. This loading may be generated by superimposing minor cycles on the major cycle dwell periods at maximum load.

When applied separately, representative major cycles give FCG rates within the Paris regime, whilst typical minor cycles give near-threshold FCG rates (da/dN_{minor}) and threshold values. The linear summation model (LSM) adds the crack growth increments due to the total stress cycle and all the minor cycles in each loading block to give a prediction of the growth rates for the CCF

*Dept of Mechanical and Manufacturing Engineering, University of Portsmouth

loading (da/dN_{CCF}). Thus:

$$da/dN_{CCF} = da/dN_{total} + (n-½)da/dN_{minor} \quad (1)$$

where n is the number of minor cycles per major cycle. The growth increment due to the total cycle (da/dN_{total}) is used since this parameter acounts ccounts for the increase in the peak-to-peak stress caused by the addition of the minor cycles to each major cycle. Figure 1 shows the model predictions for a suitably large value of n. In regime 1 da/dN_{minor} is zero; in regime 2 it is not. The transition between these regimes therefore corresponds to a threshold for minor cycle growth under CCF loading conditions. This study seeks to characterise the response of an alloy steel to CCF loadings, and to evaluate the effectiveness of the LSM in predicting the observed behaviour.

EXPERIMENTAL PROCEDURE

The readily available and widely used nickel-chromium steel 817M40 is representative of a wide range of alloy steels used in the manufacture of machine components. Its nominal composition is 0.4%C-1.55%Ni-1.15%Cr-0.6%-Mn-0.3%Mo. Austenitising at 840 °C and tempering at 650 °C generates a quenched and tempered microstructure. Typical tensile properties for 817M40 steel developed by this heat treatment, and measured at 400°C, are: a tensile strength of 860 MPa, a 0.2 % proof stress of 655 MPa, an elongation to fracture of 17 %, and a reduction of area of 65 %. Corner notched (CN) specimens with a length of 88 mm were machined from 25 mm diameter bar stock of 817M40 steel. The CN specimen (3) is a tensile loaded testpiece having a gauge length of square cross-section with a 0.3 mm deep notch centrally located along one corner.

The major cycles were represented by trapezoidal stress waves with a stress ratio (R) of 0.1, while the minor cycles were sinusoidal stress waves at a loading frequency of 150 Hz and a stress ratio of 0.9. A ratio of 1000 minor cycles per major cycle was employed; using a servohydraulic actuator to apply the major stress cycles and an electro-magnetic vibrator to supply the minor cycles. All the FCG tests were conducted at 400°C and either duplicated or triplicated. Near quarter-circular, 0.6 mm, cracks were developed in the 10 x 10 mm cross-section of the CN specimens at 400 °C using a remote tensile loading with a stress ratio of 0.1. Thereafter, for loadings involving either the application of major cycles alone or combined major and minor cycles, the FCG rates were determined as the crack grew from a length of approximately 0.6 to 5 mm. Crack length was monitored using a pulsed direct-current potential-difference method, applying the calibration obtained by Hicks and Pickard (4). Ranges of stress intensity factors (ΔK_{minor}, ΔK_{major} and ΔK_{total})

were calculated using the relationships developed by Pickard (3), and growth rates were determined by the 3-point secant method.

In each tests using minor cycles only a 0.6 mm crack was again generated in the manner described above; proir to the determination of the fatigue threshold value. In the commonly used technique the minimum load was gradually increased to give crack growth at R=0.9 (Figure 2a). Thereafter a sequence of progressive reductions in the load range at R=0.9 was used to find the step which was insufficient to sustain FCG growth above 1×10^{-8} mm/cycle. In the case of the step change or jump method for threshold determination, the crack was first grown using a loading of R=0.1. The minimum stress was then rapidly increased to give a stress ratio of 0.9 (Figure 2b). If no growth was observed the loading was returned to R=0.1 and the crack extended. This process was repeated until the loading with R=0.9 gave a growth rate of more than 1×10^{-8} mm/cycle. Following the determination of the threshold value the near-threshold growth rates were measured.

RESULTS AND DISCUSSION

The measurement of FCG rates resulting from the separate application of major cycles gives a base line against which the effects of superimposed stresses can be gauged. It also provides input data for the LSM. Figure 3 shows the plot of da/dN_{major} versus ΔK_{major}. These experimental data are represented by a scatter band, whose width corresponds to a 1.5-fold variation in growth rate at a given value of ΔK_{major}, and whose form is bi-linear, with a slope of 2.7 at stress intensity ranges below 22 MPa.m^{½}, and 2.0 above 22 MPa.m^{½} .

The tests involving the separate application of minor cycles also provide input data for the LSM. In particular, the measured threshold values are used in the prediction of the onset of minor cycle crack growth. The possible effect of load history is investigated by employing two methods of threshold determination, which involve either the gradual shedding or a step change in the applied loads. Low values of fatigue threshold are obtained with the gradual load shedding technique (Table 1).

Table 1 Minor cycle fatigue threshold values

Test method	Threshold Value (MPa m^{½})
Gradual Load Shedding	2.8, 2.9
Step Change in Loads	3.1, 3.5
Derived from CCF Transition	3.9, 3.9

Figure 4 shows the plots of da/dN_{minor} versus ΔK_{minor}. The faster near-threshold growth rates are associated with the gradual load shedding test, but all the data merge at a growth rate of approximately 1×10^{-6} mm/cycle.

When using a sufficient number of minor cycles per major cycles, crack growth measurements for CCF loadings lead to the definition of the two regimes of crack growth behaviour and the parameter ΔK_{onset} which marks the transition between them. This is demonstrated by Figure 5 in which the experimental data is plotted as da/dN_{CCF} versus ΔK_{total}. Regime 1 is bi-linear, with a slope of 2.8 at stress intensity ranges below 22 MPa.m^{½}, and 2.4 above. The transition to regime 2 occurs at 35 MPa.m^{½} when the gradient increases to 5.1.

Comparing the growth rate predictions of the LSM model with the experimental observations, tests the validity of the model and identifies the occurrence of crack growth retardations and acceleration. The predicted FCG rate curves shown in figure 6 were generated using equation 1 and da/dN data taken from figures 3 and 4. The model predictions slightly underestimate the growth rates in regime 1, and overestimate those in regime 2, whilst the transition between these two regimes is clearly underestimated, particularly by the use of minor cycle data obtained with the load shedding method.

Marci et al (5) have reported that the minor cycle threshold value obtained by the step change test method can be less than that following a gradual load shedding procedure. In particular, they observed that the reduction was greater for the nickel-based superalloy Inconel 617 than for Ti-6Al-4V plate material. Powell et al (6) have also reported a similar response for the nickel-based superalloy, Waspaloy. Additionally, they found that the threshold values generated by these test methods were greater than that associated with the onset of minor cycle growth under a CCF loading. This behaviour can be rationalised on the basis of the frequency with which the minor cycles are underloaded; which is zero in the case of a gradual load shedding test, once for a step change test, and periodically for a CCF test. This cannot be a universal explanation, since the observations for 817M40 steel contrast strongly with those of nickel based superalloys. Table 1 shows that the greatest minor cycle threshold values determined for 817M40 steel are those associated with the transition from regime 1 to regime 2 in the CCF tests. Thus for this alloy the more frequent the underloading of the minor cycles the higher was the threshold value. This is contrary to the expected behaviour associated with underloading, and so for this material, fractographic or environmental interactions are possible of greater significance. Future work will therefore examine the effect of frequency of underloading on the crack growth behaviour of his steel.

CONCLUSIONS

Fatigue crack growth rates have been measured at 400 °C in corner notched specimens of 817M40 wrought steel. The separate application of major cycles with a stress ratio of 0.1 generated a bi-linear fatigue crack growth curve. The near-threshold crack growth rates for the separate application of minor cycles at a stress ratio of 0.9 were influenced by the rapidity of the prior load shedding procedure. Under the conjoint action of major and minor stress cycles, the expected form of crack growth rate curve was observed. The linear summation model did not predict the observed growth rates, particularly when using the minor cycle data obtained with the gradual load shedding method.

REFERENCES

1. Powell B E , Int. J. Fatigue, 1995 , Vol 17, pp. 221-227.
2. Guedou, J. Y. and Rongvaux, J. M., "Effect of superimposed stresses at high frequency on low cycle fatigue", ASTM STP 942, ASTM, Philadelphia, 1988, pp. 938-960.
3. Pickard A C "The application of 3-dimensional finite element methods to fracture mechanics and fatigue life predictions", EMAS, Warley UK, 1986.
4. Hicks, M. A., and Pickard, A. C., Int. J. of Fract., 1980, Vol 20, pp. 91-101.
5. Marci, G., Castro D. E. and Bachmann V., J. Testing and Eval., 1989, Vol 17, pp. 28-39.
6. Powell, B. E., Hall, R. F. and Hawkyard. M., "The effect of superimposed vibrational stresses on fatigue crack propagation life", Conf. Struct. Integrity Assessment, Manchester, 1992, pp. 336-345.

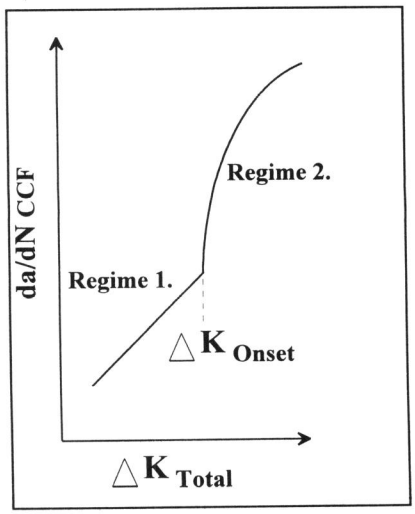

Figure 1. Anticipated crack growth for combined major and minor cycles.

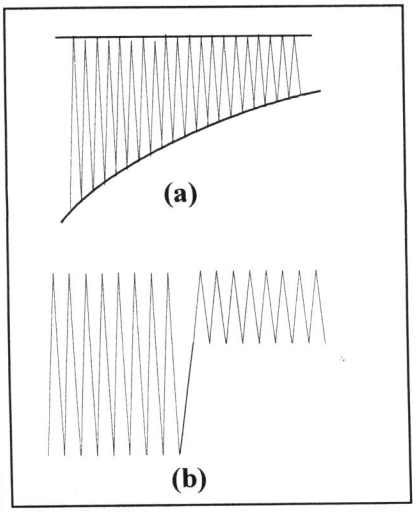

Figure 2. Loading sequences: (a) load shedding; (b) step change.

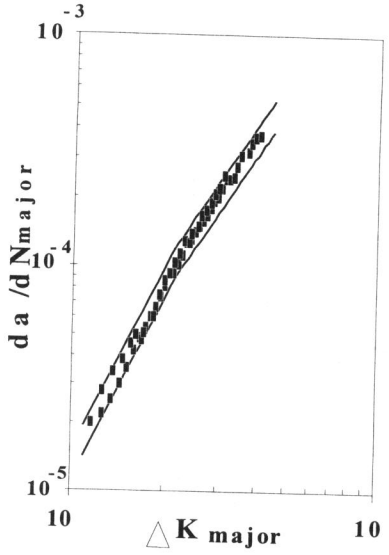

Figure 3. Fatigue crack growth rates for separate major cycles.

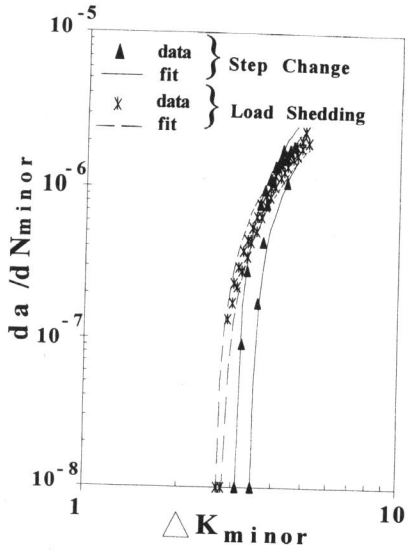

Figure 4. Fatigue crack growth rates for separate minor cycles.

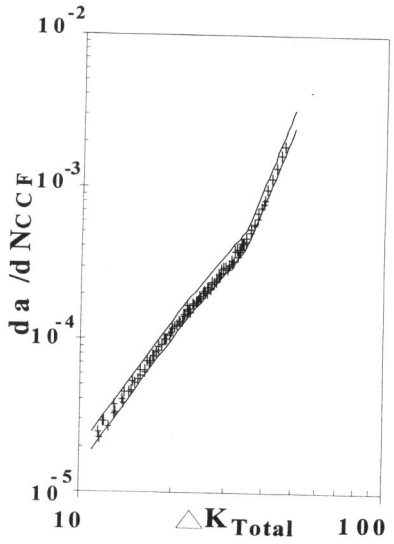

Figure 5. Fatigue crack growth rates for combined major and minor cycles.

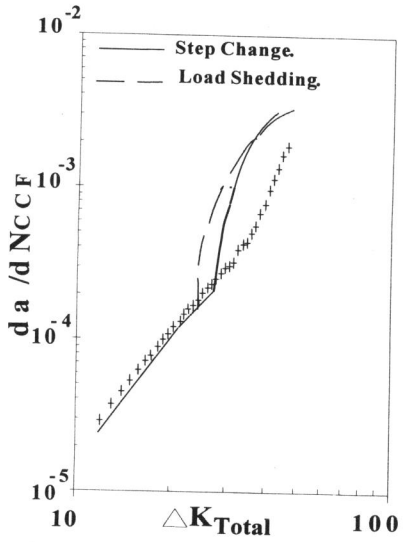

Figure 6. Comparison of experimental and predicted growth rates.